Amplification and diffusion of spontaneous emission in strongly scattering medium

Kouki Totsuka[a),b)]
Department of Physics, Faculty of Science, Shizuoka University, 836 Ohya, Shizuoka 422-8529, Japan

Gijs van Soest
Van der Waals-Zeeman Instituut, Universiteit van Amsterdam, Valckenierstraat 65, 1018 XE Amsterdam, The Netherlands

Tetsu Ito
Department of Physics, Faculty of Science, Shizuoka University, 836 Ohya, Shizuoka 422-8529, Japan

Ad Lagendijk
Van der Waals-Zeeman Instituut, Universiteit van Amsterdam, Valckenierstraat 65, 1018 XE Amsterdam, The Netherlands

Makoto Tomita
Department of Physics, Faculty of Science, Shizuoka University, 836 Ohya, Shizuoka 422-8529, Japan

(Received 27 April 1999; accepted for publication 25 February 2000)

We experimentally examined the threshold of the spectral collapse in dye embedded in a strongly scattering medium as a function of the excitation beam diameter and the transport mean free path in order to find a condition to minimize the threshold. We found a critical transport mean free path, below which the threshold pulse energy is almost independent of the mean free path. Experimental observations are well explained by a theoretical model based on the rate and diffusion equations, which shows that the luminescence spectra are also dependent on the position in the medium. © *2000 American Institute of Physics.* [S0021-8979(00)05111-2]

I. INTRODUCTION

Propagation of light in a random scattering medium has been extensively studied. The effect of absorption for light propagation is now well understood. Absorption terminates the light propagation depending on the trajectory length. The effect of absorption on the reflection and transmission coefficients, the memory effect, and the coherent backscattering peak have been studied.[1–3] Recently, amplification of light in random medium has been attracting much interest. Amplification in random scattering media exhibits a behavior totally different from absorption. Light is amplified in a random medium depending on the trajectory length. The light traveling along a long trajectory is amplified more than light in a short trajectory. Wiersma and Lagendijk reported a narrowing of the coherent backscattering peak in amplifying random media.[4]

Another interesting phenomenon in strongly scattering media may be the random laser, which has been first suggested by Letokhov as an analog of a nuclear reactor, where strong feedback is provided by scattering.[5] Lawandy *et al.* reported the observation of a spectral collapse and a shortening in the lifetime in the luminescence from colloidal suspensions containing rhodamine 640 perchlorate dye in methanol and TiO_2 particles, which resembles multimode laser behavior. This phenomenon is called random lasing. After Lawandy *et al.* reported the random laser, many experimental and theoretical studies have been reported.[6–9] The dependence of spectral and temporal characteristics of the random laser on dye concentration and density of scattering particles have been studied.[6,7] In a high dye concentration sample, bichromatic emission has been observed.[8,9] Powder lasers display similar phenomena. Gouedard *et al.* reported the multipulsing behavior in hydrated neodymium chloride powder, which is similar to the relaxation oscillation in a conventional cavity laser.[10] Noginov *et al.* reported the second harmonic powder lasers and the color center powder laser.[11,12] From the application point of view, random or powder lasers have the potential to be a unique, simple, compact, and low cost light source. It could be a new type of light source in a wide wavelength region. Random or powder lasers could be used for testing the solid state laser materials. LaRochelle *et al.* suggested the possibility for using these gain scattering media in the identification of friend and foe.[13]

Wiersma and Lagendijk categorized amplifying random medium into three regimes depending on the strength of scattering.[14] In the weak scattering regime, where the transport mean free path l^* is on the order of sample thickness, the role of scattering is only to scramble the amplified spontaneous emission. In the modest scattering regime, where l^* is much smaller than the sample size but still larger than the wavelength, the scattering increases the residence time of light in the gain region owing to the multiple scattering. As well as the present experiment and calculation, most reports so far reported on the random lasers are in this regime. We

a)Author to whom correspondence should be addressed; electronic mail: ktotsu@ohtsu.jst.go.jp
b)Present address: ERATO Ohtsu Localized Photon Project, Japan Science and Technology Corporation, 687-1 Tsuruma, Machida, Tokyo 194-0004, Japan.

could also consider the strong scattering regime, where l^* becomes equal to or smaller than the wavelength. In such a condition, the recurrent scattering event becomes more important. Recently, Cao *et al.* has reported random laser action in semiconductor powder, where the mean free path is less than the emission wavelength.[15] They observed discrete lasing modes and argued that these modes arise from ring cavities in the scattering medium formed by the recurrent scattering.

The random laser in the modest scattering is based on two competing processes: amplification and diffusion.[16] Amplification occurs in the gain region and scattering confines the luminescence in a small spatial region. If the gain volume of the luminescence light is smaller than its diffusion volume, the amplification is not efficient as the light propagates mostly through the gainless region. On the other hand, if we make the gain volume larger than the diffusion volume of the luminescence light, the excitation pulse energy is not used efficiently. Therefore we could find an optimized condition under which the pulse energy is used most efficiently for the lasing process.

In this article we systematically investigated the laser threshold as a function of the excitation beam diameter and the transport mean free path from the spectral collapse. These investigations are relevant when we consider the practical use of random or powder lasers. We found a critical transport mean free path below which the laser threshold is almost independent of the mean free path. We explain the dependence of laser threshold on excitation beam diameter and transport mean free path by numerical calculation based on diffusion and rate equations.

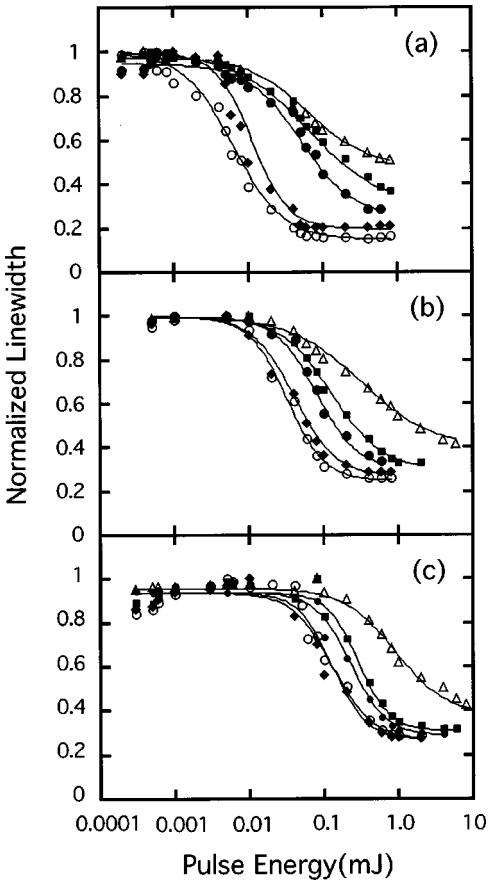

FIG. 1. Normalized linewidth as a function of the excitation pulse energy. The excitation beam diameters are: (a) 100 μm, (b) 1 mm and (c) 2 mm. The volume fractions of the polystyrene spheres are: (○) 9%, (♦) 4.5%, (●) 0.9%, (■) 0.45%, and (△) 0.09%.

II. EXPERIMENT

Spectral experiments were performed on colloidal solutions containing kiton red in methanol and polystyrene spheres. Dye concentration was 1×10^{-3} M. The absorption length was 98 μm. The scatterers used were polystyrene spheres with a diameter of 0.45 μm (Sekisui Chemical Co.). The density of polystyrene spheres varied from 0.09% to 9%, which corresponds to a transport mean free path of 2100–21 μm. The sample was pumped by linearly polarized 532 nm laser pulses from a frequency doubled Q-switched Nd^{3+} YAG laser with a pulse width of 8 ns and a pulse repetition rate of 5 Hz. The excitation pulse energy varied from 0.0001 to 8 mJ. The sample cell was cylindrical with a diameter of 11 mm. Experiments were performed on three different excitation beam diameters of 100 μm, 1 mm, and 2 mm. The luminescence spectrum from the central point of excitation beam on the incident surface was measured. The luminescence light from the sample was led to a 25 cm polychrometer and detected by a charge coupled device camera.

The luminescence from the colloidal suspensions containing kiton red showed a spectrum peaked at 585 nm with a linewidth of 30 nm upon weak excitation. The linewidth of the luminescence from the sample decreased when the excitation pulse energy was increased. Figure 1 shows the linewidth as a function of excitation pulse energy for five different sphere densities for three different excitation beam diameters: 100 μm, 1 mm, and 2 mm. We can observe several characteristic features in Fig. 1. In this figure, we see two regions for the dependence of the laser threshold on the transport mean free path. One is the region where the laser threshold increases when the transport mean free path is increased. This is seen in an all sphere density range for 100 μm beam diameter and in a low sphere density range for 1 and 2 mm beam diameters. The other is the region where the laser threshold is almost independent of the transport mean free path. This is seen above 4.5% sphere density with 1 and 2 mm excitation beam diameters. We define the laser threshold as the pulse energy at which the linewidth of the luminescence spectrum reduces to half of the initial width observed in the weak excitation limit. Figure 2 shows the threshold as a function of transport mean free path for three beam diameters. The arrows in Fig. 2 show the critical transport mean free path for each beam diameter below which the laser threshold is almost independent of the mean free path.

In Fig. 1 we see that the slope of linewidth as a function of the excitation pulse energy depends on the volume fraction of spheres. A sharp spectral collapse is seen for the sample with 9% sphere density for the excitation beam of 1 mm. The normalized linewidth decreases from 0.8 to 0.4 when the excitation pulse energy is changed from 0.015 mJ to the five times higher value of 0.08 mJ, as shown in Fig. 1(b) with open circles. On the other hand, in the case of the

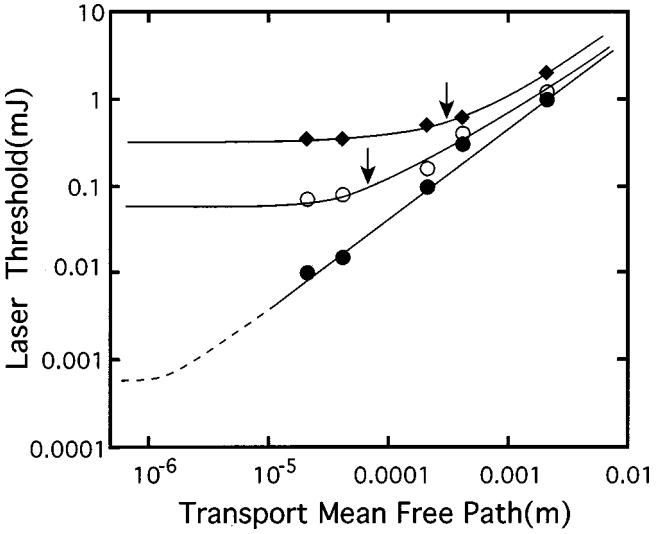

FIG. 2. The laser threshold as a function of transport mean free path. The excitation beam diameters are: (♦) 2 mm, (○) 1 mm, and (●) 100 μm. Solid lines are a guide to the reader's eye.

0.09% sphere density sample, the spectral collapse occurs slowly as a function of the excitation pulse energy. The normalized linewidth decreases from 0.8 to 0.4 when the excitation pulse energy is changed from 0.1 mJ to the 80 times higher value 8 mJ, as shown in Fig. 1(b) with open triangles. When the pulse energy is increased, we see that the linewidth slightly increases before the spectral collapse. This phenomenon could be well explained when we consider saturation absorption in the excitation process and the reabsorption in the luminescence process.[16] This tendency is most clear in the experiments with the excitation beam of 2 mm and the high sphere density sample, since much light comes around from the brim region into the central region from where the luminescence spectra are observed.

III. THEORY

To explain our experimental results, we performed a numerical calculation. In this calculation, light propagation in the medium and the excitation and emission processes were analyzed on the basis of the coupling of diffusion and rate equations. The energy states for dyes are the ground state S_0 and the excited state S_1 which consist of many vibrational and rotational sublevels. The excitation light pumps the dye molecules from S_0 to S_1. Since the nonradiative decay rates within S_0 and S_1 manifolds are very fast, we assume that the population of S_0 and S_1 are in their lowest sublevels. Then, the excited molecules emit light through spontaneous emission, which is the transition from the lowest sublevel of S_1 into vibrational sublevels of S_0. When the emitted light travels through the medium, amplification occurs owing to the stimulated emission from S_1 to S_0 depending on the local excited state population. Considering the dye molecular density is N and the populations of dye molecule in S_0 and S_1 states are N_0 and N_1, respectively, we may express the rate equation for the dye molecules as

$$\frac{\partial N_1(\mathbf{r},t)}{\partial t} = \sigma_a(\lambda_e) N_0(\mathbf{r},t) I_e(\mathbf{r},t) - \int \sigma_s(\lambda_l) N_1(\mathbf{r},t)\, \eta(\lambda_l,\mathbf{r},t) d\lambda_l - \frac{N_1(\mathbf{r},t)}{\tau}, \quad (1)$$

where the populations in dye molecules are related to $N = N_0(\mathbf{r}) + N_1(\mathbf{r})$. Here, $I_e(\mathbf{r},t)$ is the light intensity for excitation light, $\eta(\lambda_l,\mathbf{r},t)$ is the light intensity emitted from dye molecules per unit wavelength at a wavelength λ_l, $\sigma_a(\lambda_e)$ is the absorption cross section at the excitation wavelength λ_e, $\sigma_s(\lambda_l)$ is the stimulated emission cross section at luminescence wavelength λ_l, and τ is the lifetime of the excited state S_1. The width of the luminescence spectrum from the sample of 9% sphere density with 100 μm beam diameter at 1 mJ is 4 nm with its peak wavelength at 590 nm. The absorption cross section at 590 nm is small enough compared with that at 532 nm, so we can neglect the reabsorption process for simplicity. Propagation of excitation and luminescence light is calculated on the basis of the stationary diffusion equation with absorption and amplification, respectively. Wiersma and Lagendijk reported on a simulation of temporal characteristics of the luminescence light from a powdered Ti:sapphire sample with a thickness of several tens of transport mean free path.[14] In the beginning of the pump pulse, the amplification competes with the loss though the boundary. This competition and the large energy deexcitation due to amplified spontaneous emission lead to an oscillatory output of the luminescence light. In our experiment, the luminescence light was observed in the time integrated spectrum and there is a relation among the pulse duration $t_p \sim 10$ ns, lifetime of the excited state of dye $\tau \sim 3$ ns and the lifetime of photon in the medium, $\tau_d < \sim 1$ ns, that $t_p \gtrsim \tau,\ \tau_d$, and the analyses of steady state condition could be good. Diffusion equations for excitation and luminescence light can be written as

$$0 = \frac{cl^*}{3} \nabla^2 I_e(\mathbf{r}) - \sigma_a(\lambda_e) N_0(\mathbf{r}) c I_e(\mathbf{r}), \quad (2)$$

$$0 = \frac{cl^*}{3} \nabla^2 \eta(\lambda_l,\mathbf{r}) + \sigma_s(\lambda_l) N_1(\mathbf{r}) c\, \eta(\lambda_l,\mathbf{r}) + \frac{N_1(\mathbf{r})}{\tau} L(\lambda_l), \quad (3)$$

where c is the velocity of light, l^* is the transport mean free path, and $L(\lambda_l)$ is the normalized profile of the luminescence spectrum. We used a Gaussian shaped function for $\sigma_s(\lambda_l)$ and $L(\lambda_l)$ in our calculation. We assume that l^* is not dependent on the wavelength of light for simplicity. For the steady state condition, one can solve Eq. (1). The ground state population is

$$N_0(\mathbf{r}) = N \frac{1}{1 + \dfrac{I_e(\mathbf{r})}{I_s + \int \eta(\lambda_l,\mathbf{r}) \sigma_s(\lambda_l)/\sigma_a(\lambda_e) d\lambda_l}}, \quad (4)$$

where $I_s = 1/[\sigma_a(\lambda_e)\tau]$ is the saturation intensity. As shown in Fig. 3, we consider that the region $z > 0$ is filled with scattering medium with dye. The incident excitation light

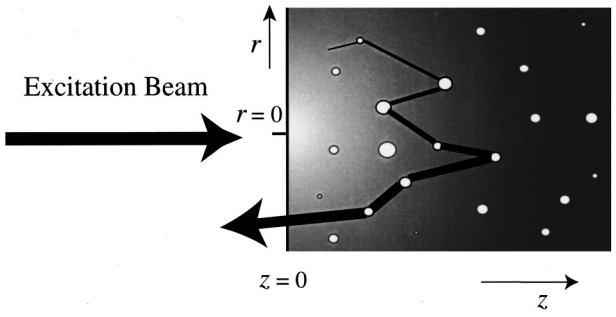

FIG. 3. Schematic illustration of the random laser.

coming from the region, $z<0$ excites the dye molecules in the sample. The luminescence light emitted by spontaneous emission undergoes multiple scattering with amplification due to the stimulated emission. The scattering only increases the residence time of luminescence light in the gain region and the recurrent scattering event is not taken into account. We calculated the luminescence light going out from the center of the excitation beam on the plane, $z=0$. As the boundary condition, we set the absorption wall at $z=-0.7l^*$.

IV. DISCUSSION

Now we compare the experimental results with the theory. We calculated excitation and luminescence processes by using Eqs. (2), (3), and (4). The parameters used in the simulation are as follows. The l^* for the sample with 9% of polystyrene spheres 0.45 μm in diameter was 21 μm. The absorption cross section $\sigma_a(\lambda_e)$ for 532 nm excitation light

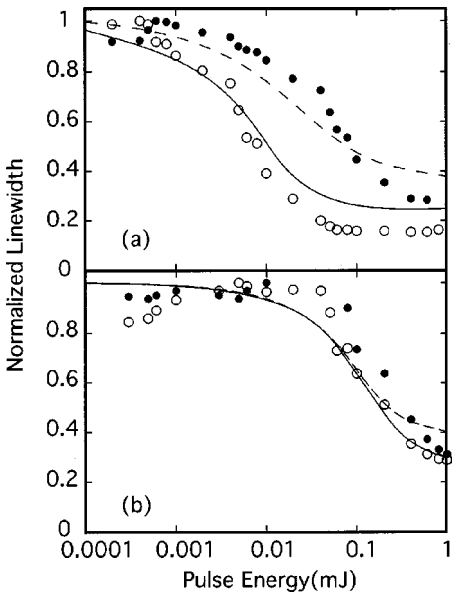

FIG. 4. Normalized linewidth as a function of the excitation pulse energy. The excitation beam diameters are: (a) 100 μm and (b) 2 mm. The volume fractions of the polystyrene spheres are: (○) 9% and (●) 0.9%. The solid and dashed lines are theoretically calculated curves for the transport mean free path of 21 and 210 μm, respectively.

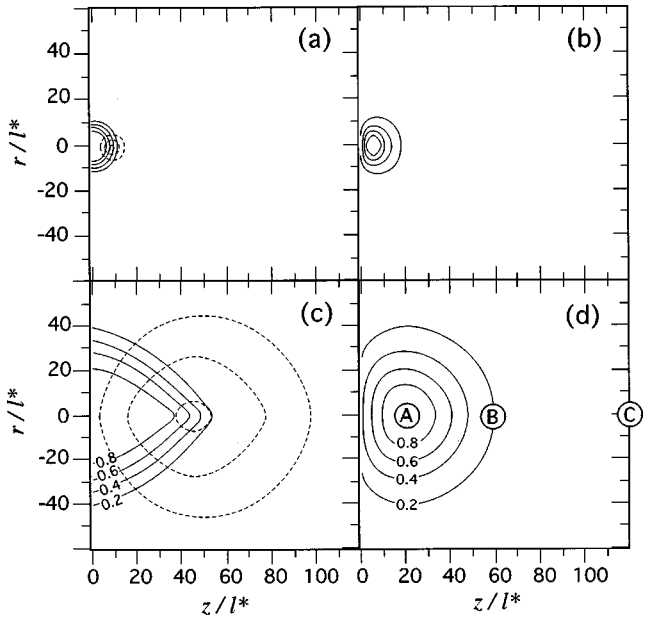

FIG. 5. (a) and (c) are calculated curves of the normalized spatial distribution of the excited state population for the excitation beam diameter of 100 μm. The transport mean free paths are: in (a) 21 μm and (c) 210 μm. Dotted lines represent the normalized spatial distribution of trajectories. Three dotted contour lines represent the intensities, 0.5, 0.1, and 0.05, toward the outside of the medium. The excitation pulse energy for (a) and (c) are 0.1 and 1 mJ, respectively. (b) and (d) are calculated curves of the normalized spatial distribution of luminescence light. Parameters are the same as in (a) and (c). The horizontal axis is the distance from the incident surface. The vertical axis is the distance from the center point of the excitation beam on the incident surface. Horizontal and vertical axes are normalized by the transport mean free path at the sphere density 9%.

was $1.7\times10^{-20}\,\mathrm{m}^2$. The excited state lifetime τ was 3.6 ns. The stimulated emission cross section $\sigma_s(\lambda_l)$ was $0.3\times10^{-20}\,\mathrm{m}^2$.

The luminescence spectrum outgoing from the incident surface is calculated. Figures 4(a) and 4(b) show the calculated and experimentally obtained linewidth as a function of excitation pulse energy for two different beam diameters. As shown in Fig. 4, calculated results recapture the experimental results. With the excitation beam of 100 μm, the laser threshold changes considerably, when the transport mean free path was changed from 21 to 2100 μm as shown in Fig. 4(a). On the other hand, with the excitation beam of 2 mm, the laser threshold is almost independent of the transport mean free path as shown in Fig. 4(b).

We analyzed the spatial distribution of the excited state population, the luminescence intensity, and the luminescence spectrum on the basis of the numerical calculation. Figures 5(a), 5(c), and 6(a), 6(c) show the normalized spatial distribution of the excited state population for the excitation beam diameter of 100 μm and 2 mm, respectively. Four solid contour lines in each figure represent the normalized intensity distribution and is drawn every 0.2 unit. The excitation pulse energies were 0.1 mJ in Fig. 5(a) and 1 mJ in Figs. 5(c), 6(a), and 6(c). Figures 5(b), 5(d) and 6(b), 6(d) show the normalized spatial distribution of the luminescence light intensity for the beam diameter 100 μm and 2 mm, respectively. The excitation pulse energies were the same as that for the figures

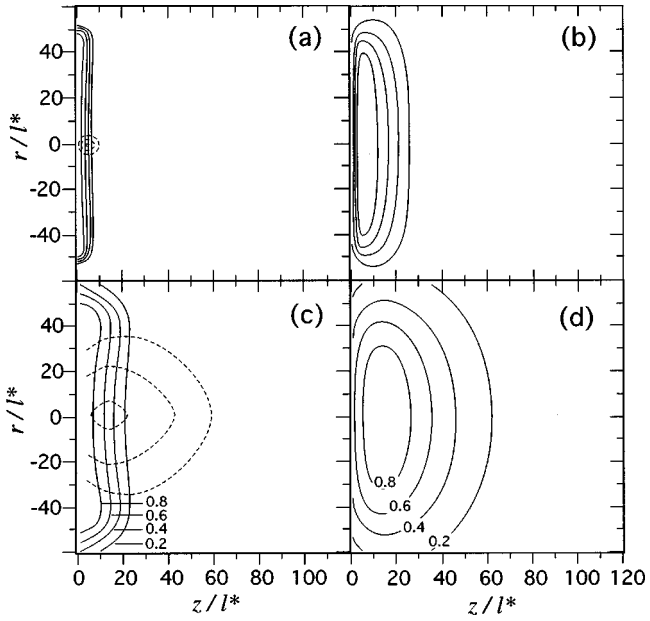

FIG. 6. All the parameters used in Fig. 6 are same as for Fig. 5 except the beam diameter and the excitation pulse energy. The excitation beam diameter and the excitation pulse energy are 2 mm and 1 mJ, respectively, for all the curves in Fig. 6.

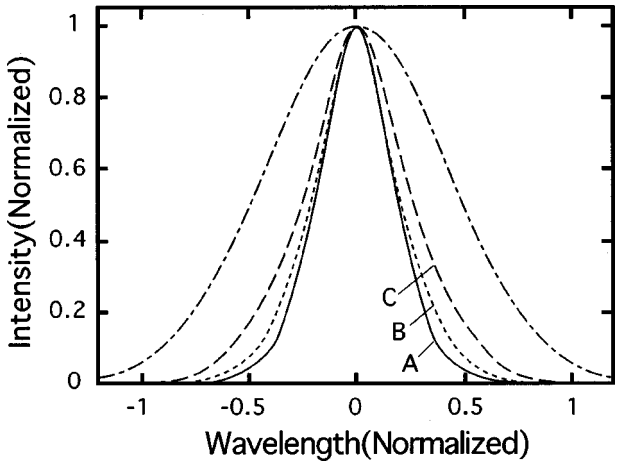

FIG. 7. Solid, dotted, and dashed lines are calculated curves of the normalized spectra inside the medium at positions (A)=20 l^*, (B)=60 l^*, and (C)=120 l^* on the z axis in Fig. 5(d). Dot-dashed line represents the original luminescence spectrum. Spectra are calculated at the excitation pulse energy of 1 mJ.

on the left hand side. With 100 μm beam diameter, the spatial distribution of excitation light intensity decays as the diffusion from a point light source. This is because the beam diameter is not large compared with the transport mean free path. With 2 mm beam diameter, the excitation light intensity decays as the diffusion from a disk light source. This is because the beam diameter is sufficiently large compared with the transport mean free path.

With increasing excitation pulse energy, the influence of the saturation absorption appears. When the saturation occurs in the excitation process, the local absorption coefficient in the vicinity of the incident surface decreases, leading to beaching in the sample. This bleaching penetrates into a deeper region with increasing excitation pulse energy.[17–19] This effect is strong with the small excitation beam since the pumping energy is concentrated in a small spatial region. As shown in Fig. 5, the spatial distribution of the excited state population also goes into the deeper region. Figures 6(c) and 6(d) show that in the $r=0$ region, the luminescence intensity is strongest, while the excited state population shows a slight dip along the central region, $r\sim 0$. This suggests strong stimulated emission in the central region.

The dotted lines in Figs. 5(a), 5(c), and 6(a), 6(c) represent typical spatial spreading of the trajectory for the luminescence light. These trajectories were calculated as a solution of the steady state diffusion equation with a launched point on the z axis, where the excited state population is half of its maximum. In these figures, we see how the two processes of amplification and diffusion are competing inside the scattering medium. The luminescence light is confined typically in the spatial region as shown with the dotted lines in Figs. 5(a), 5(c) and 6(a), 6(c). Amplification occurs in the gain regions shown in Figs. 5(a), 5(c) and 6(a), 6(c) with solid lines. If we make the gain volume larger than the diffusion volume of the luminescence light, excitation pulse energy is not used efficiently. This is the situation in Figs. 6(a) and 6(b). Most of the experiments and theoretical analyses so far reported on the random and powder lasers are performed in this condition; that is the beam diameter is larger than the transport mean free path. Let us consider a typical length for trajectories. Seed light starts to diffuse from the position $L_a=(l^* l_a/3)^{1/2}$, where L_a is the diffusive absorption length and l_a is the absorption length of the neat dye. The typical path length for this light to travel before going out from the interface surface is $L_a^2/l^*=l_a/3$, which is independent of the transport mean free path.[20] This simple discussion, which neglects the effects of the saturation absorption, excitation volume, and the reflectivity of the excitation light, explains the experimental dependence of laser threshold on the transport mean free path below the critical transport mean free path. In Fig. 2, the transport mean free path below 200 μm for the 2 mm excitation beam and the transport mean free path below 100 μm for the 1 mm excitation beam are in this condition. Figures 5(a) and 5(b) correspond to the condition that the excitation beam diameter is smaller than the diffusion volume of the luminescence light. In this case, the matching between the gain volume and the diffusion volume of luminescence light becomes worse when the transport mean free path is increased. The laser threshold increases with the transport mean free path, which is clear from Fig. 2 for a transport mean free path above 1 μm and an excitation beam of 100 μm in diameter.

The luminescence light propagates through regions with and without gain. The gain coefficient is position dependent inside the medium. The luminescence spectrum, therefore, also depends on the position in the medium. Figure 7 shows calculated curves of the normalized spectra inside the medium at positions shown in Fig. 5(d) on the z axis. At a position where the luminescence intensity is strong, the linewidth is narrow as shown in Fig. 7 with the solid line. On the other hand at a position where the luminescence intensity is weak, the linewidth is relatively broad as shown in Fig. 7

with the dotted and dashed lines. Still a considerable spectral collapse is seen by the dashed line in Fig. 7 and the linewidth is narrow compared with that expected from the local excitation population. The diffusion of the luminescence light well explains this situation.

Wiersma and Langendijk suggested that there is a critical sample thickness $L_{cr}=\pi l_{amp}$ above which the random amplifying medium is unstable.[14] When the sample size is larger than this critical size the amplification overcomes the loss due to boundary. Cao *et al.* examined the dependence of the luminescence output on the excitation beam diameter in order to compare the experimental critical beam size with the theoretical critical volume.[15] Our intention of the present experiment is to find a suitable condition to use a pulse energy most efficiently to the random laser. Still, we may describe our experimental results shown in Fig. 1 in terms of the critical volume. Let us consider the excitation condition on the basis of excitation intensity per area. An excitation condition of 0.07 mJ/mm^2 corresponds to pulse energies of 0.0007, 0.07, and 0.28 mJ for 100 μm, 1 mm, and 2 mm diameter, respectively. Let us see the luminescence from the sample of 9% of polystyrene spheres shown with open circles in Fig. 1. For the beam diameter of 100 μm, the spectrum is still broad under this excitation condition. For the beam diameter of 1 mm, the spectral width is about half of its initial value and the spectrum is collapsing. For the beam diameter of 2 mm, the width has collapsed into the final value. These results mean that the critical beam diameter which corresponds to the critical volume is 1 mm for this excitation condition.

Our present simulation shows that the threshold depends on the transport mean free path above the critical mean free path [Fig. 4(a)], while it is less dependent below the critical mean free path [Fig. 4(b)]. In Fig. 4, one may, however, notice a slight discrepancy between the simulation and the experiment in the final spectral width after the collapse. The origin of this discrepancy is not certain but it may originate in the simplicity of our model, which ignores the reabsorption effect of the luminescence light and the triplet state, etc. The reabsorption effect would obviously be important when we consider the normalized spectral linewidth since the luminescence from dye in scattering medium is narrower compared with the neat dye solution under weak excitation condition owing to the reabsorption effect. Zhang *et al.* reported that the final width depends on many parameters, such as the concentration of dye and the concentration of scatterers.[21] They argued that the laser heating and the surface area of scatterer could also influence the final width. Simulations with these parameters taken into account could figure out how these factors influence the final width. The slight spectral broadening before the spectral collapse is not seen in our calculation because we ignore the reabsorption process.

V. CONCLUSION

We observed the spectral collapse as a function of excitation pulse energy for three different excitation beam diameters in the modest scattering regime. In the modest scattering regime, the scattering increases the residence time of light in the gain region. We find that the random laser has a critical transport mean free path for each beam diameter below which the laser threshold is almost independent of the mean free path. Theoretical calculations based on the rate and diffusion equations well explain the dependence of the laser threshold on the excitation beam size and the transport mean free path. This theoretical analysis also shows that the spectrum of the luminescence light is position dependent inside the medium as the result of amplification and diffusion of the luminescence light. The critical transport mean free path would be important in a practical use of this amplifying and scattering material in applications.

ACKNOWLEDGMENTS

This research is supported by Casio Science Promotion Foundation. One of the authors (M.T.) would like to thank Dr. M. Kroon for interesting discussions and for his kind hospitality at University of Amsterdam.

[1] A. Z. Genack, in *Scattering and Localization of Classical Waves in Random Media*, edited by P. Sheng (World Scientific, Singapore, 1990).
[2] M. Tomita, Phys. Rev. B **45**, 1045 (1992).
[3] S. Etemad, R. Thompson, M. J. Andrejco, S. John, and F. C. MacKintosh, Phys. Rev. Lett. **59**, 1420 (1987).
[4] D. S. Wiersma and Ad Lagendijk, Phys. Rev. Lett. **75**, 1739 (1995).
[5] R. V. Ambartsumyan, P. G. Krykov, and V. S. Letokhov, Sov. Phys. JETP **24**, 1129 (1967).
[6] N. M. Lawandy, R. M. Balachandran, A. S. L. Gomes, and E. Sauvain, Nature (London) **368**, 436 (1994).
[7] M. Siddique, R. R. Alfano, G. A. Berger, M. Kempe, and A. Z. Genack, Opt. Lett. **21**, 450 (1996).
[8] W. L. Sha, C.-H. Liu, F. Liu, and R. R. Alfano, Opt. Lett. **21**, 1277 (1996).
[9] S. John and G. Pang, Phys. Rev. A **54**, 3642 (1996).
[10] C. Gouedard, D. Husson, and C. Sauteret, J. Opt. Soc. Am. B **10**, 2358 (1993).
[11] M. A. Noginov, S. U. Egarievwe, N. E. Noinova, J. C. Wang, and H. J. Caulfield, J. Opt. Soc. Am. B **15**, 2854 (1998).
[12] M. A. Noginov, N. E. Noinova, S. U. Egarievwe, H. J. Caulfield, P. Venkateswarlu, A. Williams, and S. B. Mirov, J. Opt. Soc. Am. B **14**, 2153 (1997).
[13] S. LaRochelle, P. Mathieu, V. Larochelle, and J. Dubois, in *Proceedings of the Conference on Lasers and Electro-Optics*, OSA Technical Digest Series, Vol. 11 (Optical Society of America, Washington, D. C., 1997), p. 143.
[14] D. S. Wiersma and Ad Lagendijk, Phys. Rev. E **54**, 4256 (1996).
[15] H. Cao, Y. G. Zhao, S. T. Ho, E. W. Seelig, Q. H. Wang, and R. P. H. Chang, Phys. Rev. Lett. **82**, 2278 (1999).
[16] G. van Soest, M. Tomita, and A. Lagendijk, Opt. Lett. **24**, 306 (1999).
[17] K. Totsuka, M. A. I. Talukder, M. Matsumoto, and M. Tomita, Phys. Rev. B **59**, 50 (1999).
[18] K. Totsuka and M. Tomita, Phys. Rev. B **59**, 11139 (1999).
[19] K. Totsuka, M. A. I. Talukder, and M. Tomita, J. Phys. Soc. Jpn. **68**, 307 (1998).
[20] A. Z. Genack and J. M. Drake, Nature (London) **368**, 400 (1994).
[21] W. Zhang, N. Cue, and K. M. Yoo, Opt. Lett. **20**, 961 (1995).